引用格式：DENG Wei，DAI Pan，WANG Feng，et al. FBG Sensor System without Wavelength Correction Based on REC-DFB Tunable Laser[J]. Acta Photonica Sinica，2023，52(12)：1206004
邓韦，戴攀，王峰，等．基于REC-DFB可调谐激光器的无波长校正FBG传感系统[J]．光子学报，2023，52(12)：1206004

基于REC-DFB可调谐激光器的无波长校正FBG传感系统

邓韦[1,2]，戴攀[2]，王峰[2]，葛涵天[2]，陈向飞[2]
（1 南京信息职业技术学院 网络与通信学院，南京 210023）
（2 南京大学 现代工程与应用科学学院，南京 210023）

摘　要：提出了一种无波长校正的光纤布拉格光栅(FBG)传感系统，可在未对基于重构等效啁啾(REC)技术制造的扫频DFB激光器进行波长线性校正的情况下，识别波长变化，并解调出光栅传感器的温度变化。所提无波长校正FBG传感系统可以在200 ℃范围内进行精确的温度检测，测得的波长与温度的线性系数$1-R^2$仅为0.004 4。该传感系统光源在1 kHz的锯齿波调制下，调谐范围可达2.5 nm，且测量过程中无需额外波长校正器件。

关键词：光纤布拉格光栅；重构等效啁啾技术；分布式反馈激光器；无波长线性校正；可调谐激光器
中图分类号：TN29　　**文献标识码**：A　　**doi**：10.3788/gzxb20235212.1206004

0 引言

随着光纤通信与光纤传感的快速发展，光纤布拉格光栅(Fiber Bragg Grating，FBG)传感器成为发展最快、应用最广的光纤传感器。由于FBG传感器具有结构小巧、造价低廉、采用波长编码、抗电磁干扰、易于复用等诸多优势，在传感领域受到广泛关注并大量应用于人体医学、压力检测、电池情况及建筑结构健康等安全监测中[1-4]。

FBG传感器通过检测FBG反射波长的变化，对应力、振动及温度等参量进行解调。其核心是光源与解调技术。FBG传感系统主要有两种波长解调方式，一是采用宽带放大自发辐射(Amplified Spontaneous Emission，ASE)光源，同时使用CCD分光计法[5]、匹配FBG可调滤波检测法[6]、非平衡M-Z干涉仪检测法[8]、可调谐光纤F-P滤波器检测法[7-9]等对FBG的波长进行检测。但是ASE光源的功率密度相对较低，并且解调系统也复杂。随着光子集成技术的不断发展，为FBG解调系统的集成化、性能进一步优化和成本进一步降低提供了可能。近年来提出的基于阵列波导光栅(Arrayed Waveguide Grating，AWG)的FBG解调系统依靠相对强度进行解调，可实现高速解调，但系统组成较为复杂且受AWG的信道间隔、串扰、插入损耗和带宽影响，与现有基于AWG的解调系统的动态范围、波长分辨率和解调精度会相互制约[10,11]。另一种方式是采用可调谐激光器光源[12-15]，这种光源具有信噪比高、线宽窄、功率密度大的特点。在扫描激光器波长的同时，利用光电探测器探测FBG反射光的强度，即可实现对中心波长的解调。目前这种基于波长扫描的FBG解调系统已经成为最流行的FBG传感解调系统之一。分布式反馈(Distributed Feedback，DFB)激光器作为一种单片集成式的可调谐半导体激光器，由于其具有单模稳定性好、输出功率大、直接调制性能好等优势已成为光通信应用中的重要组成部分。然而，目前面向光通信应用需求的可调谐DFB激光器往往调谐范围较窄、调谐速率低，且直接作为传感解调系统使用时需要额外辅助的波长参考基准，这就导致系统复杂，影响了它的实用性。因此，目前还没有一种结构简单、低成本的面向FBG传感系统专门适用的可调谐激光器光源。

基金项目：国家自然科学基金(No. 61975076)，国家重点研发计划(Nos. 2018YFA0704402，2018YFB2201801，2018YFE0201200)
第一作者：邓韦，dengwei@njcit.cn
收稿日期：2023-05-19；**录用日期**：2023-08-23

本文以自主研制的基于重构等效啁啾(Reconstruction-Equivalent-Chirp,REC)技术设计并制备的DFB激光器为光源,提出了一种无需(辅助波长参考系统)波长校正系统的FBG温度传感系统,它具有测量范围宽、调谐速率高、测量精度高、系统成本低等优点。激光器光源能以1 kHz的扫描速率实现2.5 nm内的连续波长调谐,且测量过程中无需额外波长校正器件,在实验中实现了200 ℃范围内的精确温度传感测量。

1 原理与设计

1.1 光纤光栅温度传感原理

FBG的光学特性表现为一个以布拉格波长为中心的窄带反射滤波器,入射光波长在FBG的布拉格波长附近会被反射,其余的光则会透射出去。布拉格波长与光栅参量的关系为

$$\lambda_B = 2\Lambda n_{eff} \tag{1}$$

式中,λ_B为反射光的峰值波长,也称布拉格波长。Λ和n_{eff}分别是光栅周期和FBG的有效折射率。

当外界温度施加在FBG上时,温度通过热光效应和热膨胀效应会影响FBG的有效折射率和光栅周期,导致布拉格波长漂移,波长偏移量表示为

$$\Delta\lambda_B = k_T \Delta T + C \tag{2}$$

式中,ΔT是温度的变化量,k_T是FBG的热灵敏系数,C是常数。由式(2)可知,当FBG受到外界温度变化的影响时,其布拉格波长也会发生偏移,并且$\Delta\lambda_B$与ΔT之间为线性关系,典型值为0.01 nm/℃[16]。

1.2 DFB激光器波长调谐原理

DFB半导体激光器作为一类重要的波长可调激光源,具有可靠性高、噪声低、响应速度快、输出功率高、重复性好、调谐方式简单等特点,并且其制造工艺相对在众多方案的可调谐激光器中,DFB激光器是兼顾成本和应用性的最佳选择。如图1所示,DFB激光器的基本结构主要由有源区、光场限制层以及光栅层组成,其中有源区为DFB激光器提供增益,光场限制层类似于光纤中的包层,用于限制激光器芯片内部的光场分布。

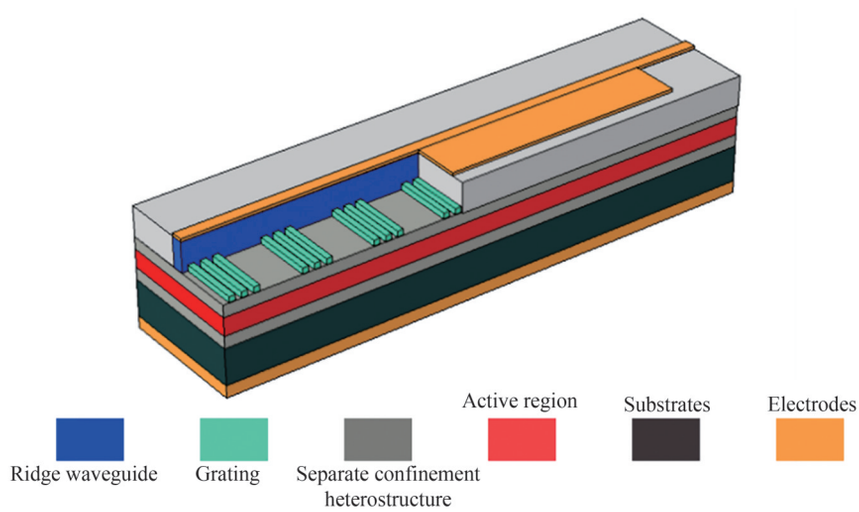

图1 DFB激光器的基本结构示意图

Fig.1 Schematic diagram of the basic structure of DFB laser

折射率耦合型DFB激光器的谐振腔为布拉格光栅,光栅的布拉格波长即为DFB激光器的激射波长。当改变注入电流时,DFB激光器的中心波长会在电流的热效应与载流子效应的影响下发生漂移。电流的热效应原理为:当注入电流增大时,由于焦耳热效应与有源区产热的影响使激光器内部温度升高[17],导致光栅层的有效折射率n_{eff}增大,根据式(1)可知,布拉格波长会随着有效折射率的增大而增大,使激光器的激射波长发生红移。载流子效应的原理为:激光器内部载流子浓度随注入电流的增大而增加,引起增益系数等参数上升,导致激光器的有效折射率下降,使光栅层的布拉格波长减小,即DFB激光器的激射波长发生蓝移。通常情况下,激光器热效应对激射波长的影响较大,但受激光器内部热容影响,热效应对注入电流的响应较慢;而载流子效应对波长的影响较小,相比热效应对波长的影响通常会小2~3个数量级,但响应速度极快。

当驱动电流变化速率较低时，激光器的电流调谐以热效应为主，其激射波长会随电流的增大而红移；而当电流变化速率较高时，激光器的电流调谐速率以载流子效应为主，其激射波长随电流的增大而蓝移。

理想情况下，DFB激光器的激射波长会随着注入电流呈线性变化。然而在实际调谐过程中，由于电流的热效应和载流子注入效应的共同影响，DFB激光器的瞬时输出波长与注入电流之间存在一定的非线性，且非线性会随着调谐速率的上升而变得愈发明显[18]，这种非线性变化增大了后续系统解调的难度。

本文使用的DFB激光器设计制备时采用了一种特殊的工艺方法—重构等效啁啾(Reconstruction-Equivalent-Chirp，REC)技术，对均匀周期的种子光栅进行采样，使工艺成本较低的亚微米量级的全息曝光技术在保留其固有特点的同时，在波长精度上达到与成本高昂的纳米级电子束曝光技术相同的效果。如图2(a)所示，REC技术先通过全息曝光制作出周期均匀的种子光栅，然后利用紫外光刻技术对种子光栅进行采样。如图2(b)所示，根据傅里叶展开理论，取样后的光栅会有0级，±1级，±2级……，±n级子光栅，再通过合理设计可以让某一级子光栅落在激光器的增益带宽内，而其它级子光栅则落在增益区外，这样DFB激光器的出射光谱特性就直接与该级子光栅相关，而子光栅的光谱特性则可以通过设计采样图形直接进行修改和优化。因此，REC技术可以在不改变种子光栅的情况下，只改变采样图形的取样周期实现对激光器波长的改变，并且由于采样周期为微米量级，因此对工艺精度的要求大为降低。前期理论和实验已经证明REC技术在制作光栅的工艺中，容差度比传统技术高两个数量级以上，这体现了REC技术对布拉格波长的精准控制[19]。

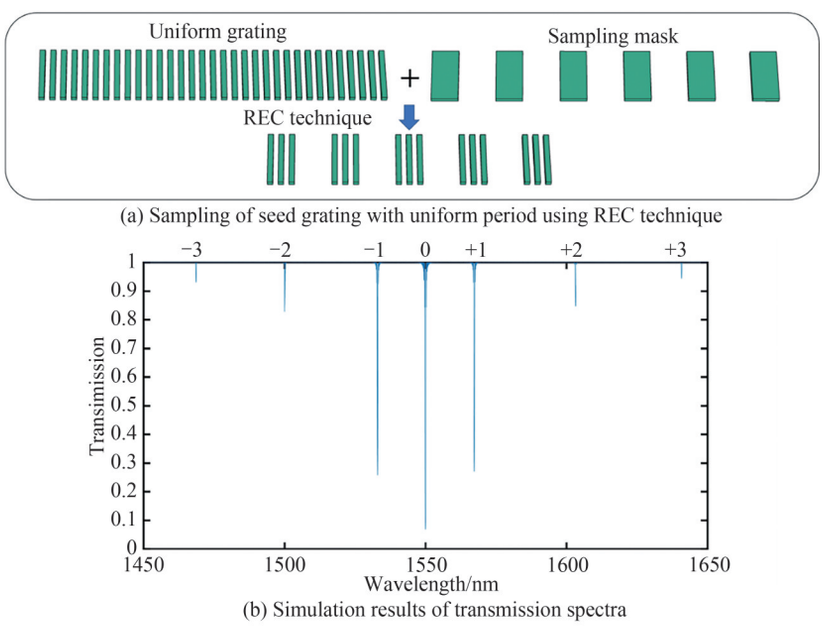

图2　采样光栅示意图与其透射谱仿真结果

Fig.2　Schematic diagram of sampling grating and simulation results of its transmission spectra

1.3　系统解调方法

当选用可调谐DFB激光器作为FBG温度传感系统光源时，通过读取经FBG反射后的信号光经过光电探测器的电压信号来对温度信息进行解调，解调原理如图3所示。FBG和DFB激光器的反射谱函数$R(\lambda)$和光谱函数$D(\lambda)$可以近似认为符合高斯分布

$$R(\lambda)=R_0\exp\left[-\frac{\ln 2(\lambda-\lambda_F)^2}{\omega_F^2 t}\right] \tag{3}$$

$$D(\lambda)=R_0\exp\left[-\frac{\ln 2(\lambda-\lambda_D)^2}{\omega_D^2}\right] \tag{4}$$

式中，λ_F是FBG的中心波长，ω_F是FBG的3 dB带宽，λ_D是DFB激光器的中心波长，ω_D是激光器输出光的3 dB带宽[20]。

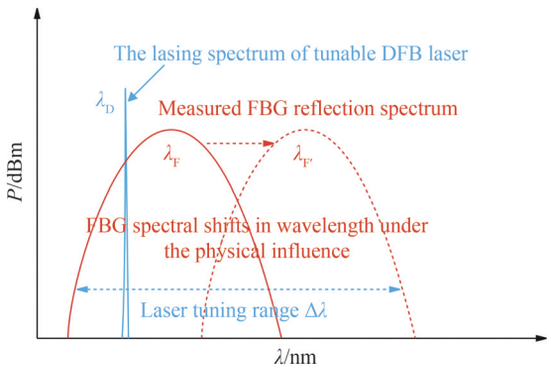

图3 可调谐DFB激光器解调原理示意图

Fig.3 Schematic diagram of FBG demodulation principle based on tunable DFB laser

因为DFB激光器输出激光的线宽远小于FBG的3 dB带宽，所以DFB激光器输出光对于FBG光谱相当于单位脉冲响应函数。因此，由FBG反射后的扫描光经过光电探测器后，信号输出为

$$V(\lambda_D)\propto R(\lambda_D\lambda)*D(\lambda_D)=\int_{-\infty}^{\infty}R(\tau)\cdot D(\lambda_D-\tau)\,d_\tau=V_0\exp\left[-\frac{\ln 2(\lambda_D-\lambda_F)^2}{\omega_F^2}\right] \tag{5}$$

式中，V_0是$\lambda_D=\lambda_F$时光电转换及放大电路的输出电压。由式(5)可知，光电转化及放大电路的输出电压的大小取决于λ_D与λ_F的差值。当$\lambda_D=\lambda_F$时，差值为零，此时DFB激光器的中心波长和FBG的反射峰重合，光电转换及放大电路的输出电压达到最大值。因此在解调系统中，可以通过读取最大电压在一个周期内的时间信息来解调出FBG中心波长和被测物理量。

2 系统与实验

在基于波长扫描的FBG传感解调系统中，能够直接从示波器(Oscilloscope，OSC)上获得的数据仅有FBG反射峰的峰值强度以及在DFB激光器扫描周期中的对应时间。要能够从这些数据中准确分析出FBG传感器测量的外界环境变化，需要提前对DFB激光器扫频过程中波长随时间的变化关系进行标定。本文首先采用基于马赫曾德尔干涉仪(Mach-Zehnder Interferometer，MZI)的标定方法标定出瞬时波长，得到波长随时间的变化关系。然后根据系统中OSC测量的电信号反射峰的具体时刻位置，得到FBG反射峰的波长信息。最后检测FBG反射光波长的偏移量，实现即使在波长非线性变化的情况下，也可以线性解调出外界待测温度的变化。

2.1 波长标定系统与实验

在FBG传感系统的解调部分中，读取OSC上得到的FBG反射峰在DFB激光器扫描周期中的时间，结合激光器的激射波长的周期性变化曲线计算出FBG反射峰位置，从而进一步得到温度信息。因此在解调前需要对DFB激光器扫频过程中波长随时间变化的关系进行标定。

基于MZI可以实现对波长的定标，该系统结构简单、具有带通和梳妆滤波等特点，被广泛应用于传感解调、全光波长转换等领域。图4中蓝色虚框内为基于MZI的扫频激光器的瞬时波长变化测量系统图，整个系统包括：可调谐激光器光源、隔离器、两个3 dB光耦合器(Optical Coupler，OC)、偏振控制器(Polarization Controller，PC)、可调衰减器、光电探测器和示波器。

为了降低偏振噪声对测量结果的影响，测量系统里面的全套光纤为保偏光纤，可以使测量系统达到最佳的干涉效果。激光器发出的扫频激光被第一个耦合器(OC1)一分为二。一路信号进入信号臂，通过调节偏振控制器使二者的偏振态相同从而达到最佳的相干效果；另一路信号进入参考臂，通过调节可调谐衰减器使得两臂的光强一致来提高干涉信号的信号对比度。两路信号在第二个耦合器处(OC2)发生干涉，最后合成的干涉光信号被光电探测器接收后送往示波器显示。

此时，MZI系统输出的光强可以表示为

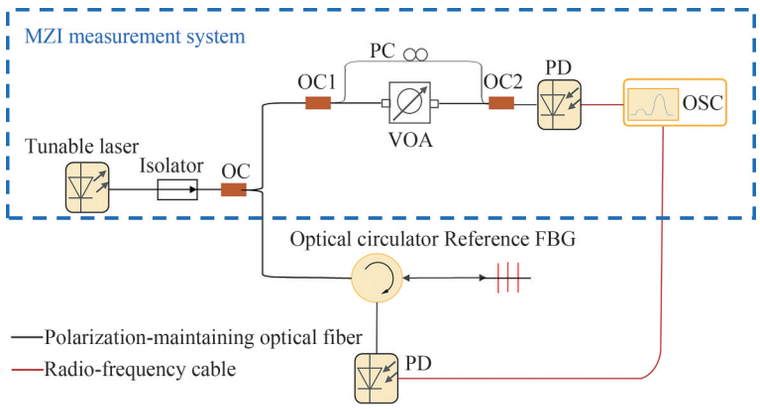

图4　基于MZI的扫频激光器的瞬时波长变化测量系统

Fig.4　Schematic diagram of the MZI-based instantaneous-wavelength-variation measurement system of frequency-swept laser

$$I_1=\frac{\alpha}{2}I_0(1-\cos\varphi)=\frac{\alpha}{2}I_0\left(1-\cos\frac{2\pi n_{\text{eff}}\Delta L}{\lambda}\right) \tag{6}$$

式中，α为出射光经过系统后的损耗系数，ΔL为信号臂与参考臂的臂长差，λ是DFB激光器的瞬时波长，I_0是DFB激光器的光功率。从式(6)中可以看出，MZI系统的输出光强度是一个随着激光器的激射波长变化的正弦函数。

当波长变化量远小于激射波长时，则示波器上相邻两个正弦波峰之间对应的波长差可表示为

$$\Delta\lambda=\frac{\lambda^2}{n_{\text{eff}}\Delta L} \tag{7}$$

在已知MZI系统的臂长差和光纤有效折射率的情况下，通过标定每个正弦峰在一个周期内的时间位置来计算激光器激射波长的相对变化曲线。为了获得激光器激射波长的绝对值变化曲线，在系统中额外加入了一段中心波长已知的参考FBG，通过读出经过参考FBG反射后的光信号在一个周期中最大值所在的时刻，推算此时刻的波长绝对值，再结合MZI系统中得到的激射波长相对变化曲线，即可得到一个扫描周期内的波长的绝对值变化曲线。

实验中，DFB激光器采用半导体制冷器(Thermoelectric Coolers，TEC)控温，温度设置在25 ℃，驱动电流为1 kHz的锯齿波电流信号，电流变化范围为80～280 mA，参考FBG中心波长为1 519.85 nm，调谐过程中激光器波长连续变化，单模特性良好且无模式跳变。MZI系统的臂长差为3 cm，经过系统后的示波器波形如图5(a)所示，对波长标定后，结合参考FBG在单个扫频周期中的时间位置，可以得到DFB激光器在扫

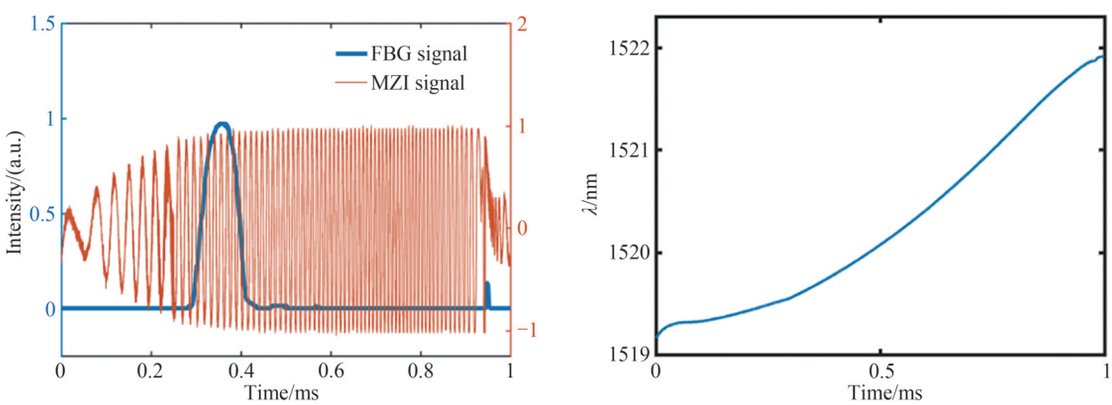

(a) The signal measured by the MZI system and the reflection signal of the reference FBG in a single frequency-swept period

(b) The relationship between laser wavelength and time

图5　单个扫频周期内经过MZI系统测得的信号与参考FBG的反射信号以及激光器波长随时间变化的关系

Fig.5　The relationship between the signal measured by MZI system and the reflection signal of reference FBG and the variation of laser wavelength with time in a single frequency-swept period

描过程中波长变化的具体范围以及对应的不同时刻的波长绝对值，处理后的实验结果如图5(b)所示。结果显示，DFB激光器在1 kHz的调制速率下波长变化大于2.5 nm。

同时为了能更直观地表征激光器的波长扫频范围，除了利用MZI系统精确测量外，还用光谱分析仪测量了激光器的扫描光谱，如图6所示。

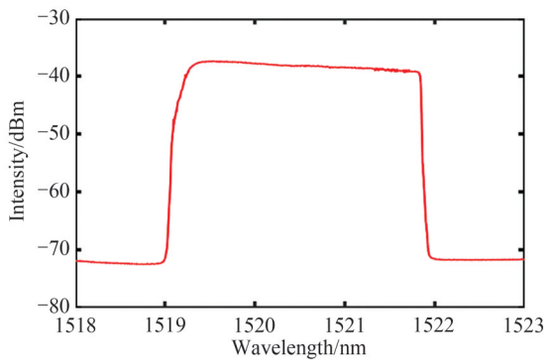

图6 光谱仪测得的激光器扫描光谱

Fig.6 Wavelength-swept spectra of laser measured by optical spectrum analyzer

2.2 温度传感系统与实验

基于可调谐激光器的FBG温度传感系统组成如图7所示，光纤光栅传感器置于恒温箱中，恒温精度0.1 ℃。实验中使用REC-DFB半导体可调谐激光器作为扫频激光光源，光信号经环形器后，作用于FBG传感器用于温度传感，随后FBG反射光信号经环形器被光电探测器接收后用示波器记录。利用激光器的输出波长与被测FBG的反射中心波长重合时反射光信号最大的特征，再利用已经标定的激光扫描周期内输出波长与时间的关系，提取解调系统FBG输出最大信号对应的波长。

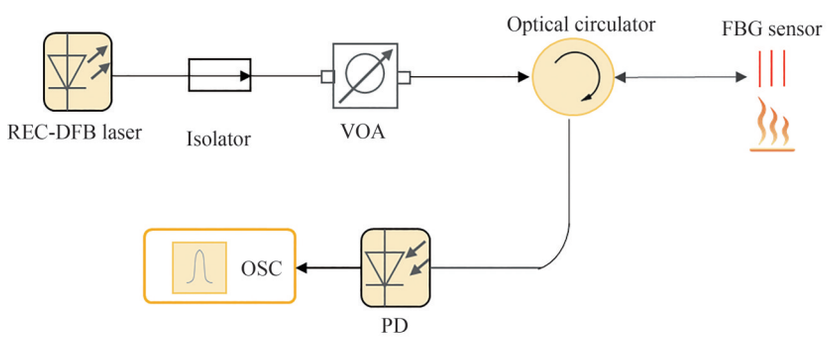

图7 基于REC-DFB可调谐激光器的FBG温度传感系统

Fig.7 Schematic diagram of FBG temperature sensing system based on tunable REC-DFB laser

搭建如图7所示的实验系统，FBG反射后从示波器上可以看到反射峰的具体时刻，这个时刻与具体波长的关系已经在图5(b)中标定。这样就可以得到温度和波长之间的关系。

温度传感实验中，将设定温度从30 ℃以5 ℃为步进逐渐加热到235 ℃，为验证传感测量重复性，在每个温度下每隔10 min后记录一次数据，即每个温度下重复记录5组数据。其中以30 ℃、60 ℃、90 ℃、120 ℃、150 ℃和180 ℃的测试数据为例，经过FBG反射后的扫频光经过PD后在示波器上的电压信号如图8(a)所示，可以看出FBG的反射峰位置随着温度的升高而往长波移动，通过读取反射峰的峰值对应的时间，结合单个周期内波长随时间的变化曲线便可以读取出此时的反射峰峰值。以此为例进行多次测量误差分析，图8(b)是重复实验过程中不同温度下的FBG反射峰峰值(滤波后)换算对应的波长，30 ℃～180 ℃由低到高不同温度下的标准差分别为9.4 pm、5.9 pm、8.5 pm、9.6 pm、6.3 pm和5.0 pm，经过误差分析表明不同温度下的测量重复性良好。

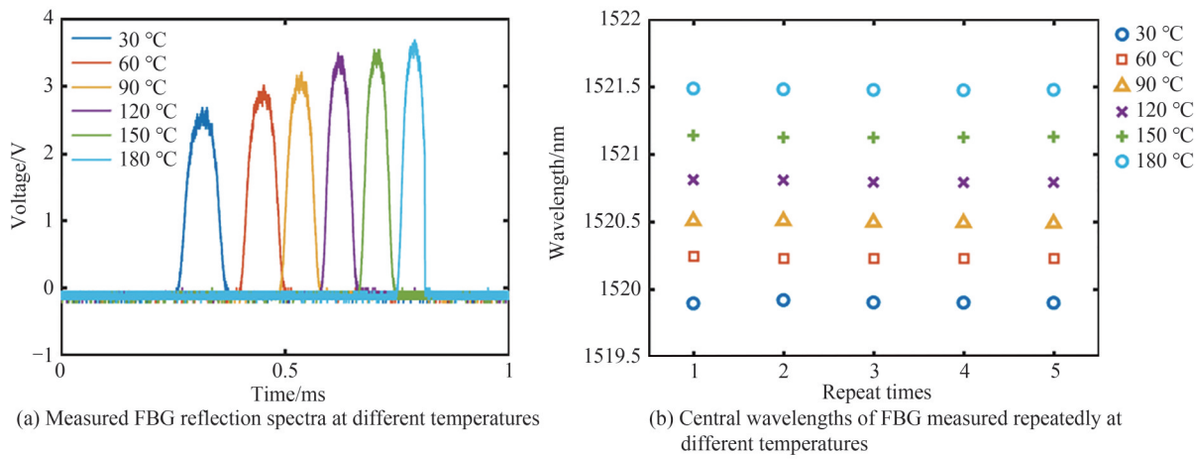

(a) Measured FBG reflection spectra at different temperatures

(b) Central wavelengths of FBG measured repeatedly at different temperatures

图8　不同温度下测得的FBG反射谱波形和多次重复测得的FBG中心波长

Fig.8　FBG reflection spectra and FBG central wavelengths measured repeatedly at different temperatures

然后用相同方法处理30 ℃～235 ℃所有42个温度点的数据：读取不同温度下反射峰峰值的时间位置并计算峰值波长、都取5次重复测试的平均值后再拟合曲线，不同温度下的峰值波长与线性拟合结果如图9所示，拟合曲线的斜率为0.010 2 nm/℃，符合FBG反射峰随温度变化的漂移系数。测试结果线性度良好，$1-R^2=0.004\ 4$，其中R^2为线性回归系数。

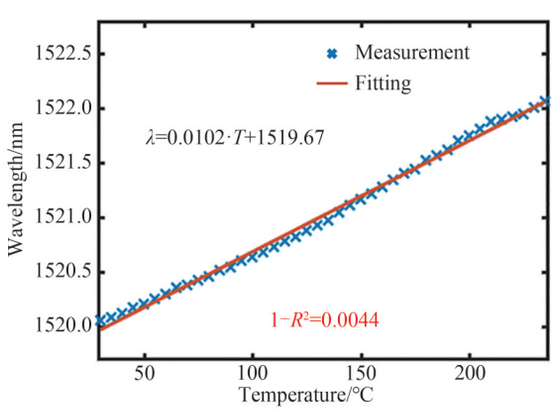

图9　不同温度下测量的FBG反射波长及其线性拟合关系

Fig.9　FBG central wavelengths measured at different temperatures and their linear fitting relationship

根据相关文章报导，将本文提出的FBG温度传感系统的关键参数与其他文章中的结果进行对比，对比结果如表1所示。

表1　几种不同的FBG温度传感系统关键参数对比

Table 1　Comparison of key parameters of several different FBG temperature sensing systems

Is wavelength correction required	Temperature measurement range	References	Linear coefficient R^2
No	200 ℃	This work	0.995 6
No	15 ℃	[21]	0.996 0
No	10 ℃	[22]	0.990 5
Yes	40 ℃	[23]	The error is less than 0.1 ℃

3　结论

提出了一种基于REC-DFB可调谐激光器的无波长校正FBG传感系统。以基于REC技术制造的DFB激光器为光源，无需波长校正系统即可实现FBG温度解调。温度实验中，激光光源能以1 kHz的扫描速率

实现2.5 nm范围内的连续波长调谐,且测量过程中无需额外波长校正器件,初步实验实现了200 ℃范围内的精确温度测量。

参考文献

[1] MASSARONI C, ZALTIERI M, LO P D, et al. Fiber Bragg grating sensors for cardiorespiratory monitoring: a review [J]. IEEE Sensors Journal, 2021, 21(13): 14069-14080.

[2] EE Y J, TEY K S, LIM K S, et al. Lithium-ion battery state of charge (soc) estimation with non-electrical parameter using uniform Fiber Bragg Grating (FBG)[J]. The Journal of Energy Storage, 2021, 40(2):102704.

[3] MIELOSZYK M, MAJEWSKA K, OSTACHOWICZ W. Application of embedded fiber Bragg grating sensors for structural health monitoring of complex composite structures for marine applications[J]. Marine Structures, 2021, 76(3): 102903.

[4] FU Z, YANG D, YE W, et al. Widely tunable compact erbium-doped fiber ring laser for fiber-optic sensing applications [J]. Optics & Laser Technology, 2009, 41(4): 392-396.

[5] HU Y, CHEN S, ZHANG L, et al. Multiplexing Bragg gratings using combined wavelength and spatial division techniques with digital resolution enhancement[J]. Electronics Letters, 1997, 33(23): 1973-1975.

[6] DAVIS M A, KERSEY A D. Matched-filter interrogation technique for fiber Bragg grating arrays[J]. Electronics Letters, 1995, 31(10): 822-823.

[7] SONG M, YIN S, RUFFIN P B. Fiber Bragg grating strain sensor demodulation with quadrature sampling of a Mach-Zehnder interferometer[J]. Applied Optics, 2000, 39(7): 1106-1111.

[8] KERSEY A D, BERKOFF T A, MOREY W W. Multiplexed fiber Bragg grating strain-sensor system with a fiber Fabry-Perot wavelength filter[J]. Optics Letters, 1993, 18(16): 1370-1372.

[9] YU Y L, TAM H Y, CHUNG W H. Technique for fiber Bragg grating array interrogation with a tunable Fabry-Perot filter [J]. Chinese Journal of Lasers, 2000, 27(12): 1103-1106.
余有龙, 谭华耀, 锺永康. 基于可调F-P滤波器的光纤光栅传感器阵列查询技术[J]. 中国激光, 2000, 27(12): 1103-1106.

[10] MOON H M, KWAK S C, IM K, et al. Wavelength interrogation system for quasi-distributed fiber Bragg grating temperature sensors based on a 50-GHz array waveguide grating[J]. IEEE Sensors Journal, 2018, 19(7): 2598-2604.

[11] NIEWCZAS P, WILLSHIRE A J, DZIUDA L, et al. Performance analysis of the fiber Bragg grating interrogation system based on an arrayed waveguide grating[J]. IEEE Transactions on Instrumentation and Measurement, 2004, 53 (4): 1192-1196.

[12] YUN S H, RICHARDSON D J, KIM B Y. Interrogation of fiber grating sensor arrays with a wavelength-swept fiber laser[J]. Optics Letters, 1998, 23(11): 843-845.

[13] HILL D J, HODDER B, DE FREITAS J, et al. DFB fiber-laser sensor developments[C]. 17th international Conference on Optical Fiber Sensors, SPIE, 2005, 5855: 904-907.

[14] SHAO L Y, DONG X, ZHANG A P, et al. High-resolution strain and temperature sensor based on distributed Bragg reflector fiber laser[J]. IEEE Photonics Technology Letters, 2007, 19(20): 1598-1600.

[15] WANG Xiaona, WANG Qi, CHEN Lehua, et al. Swept fiber laser based fiber optic sensor demodulator[J]. Acta Photonica Sinica, 2009, 38(1): 82-86.
王晓娜, 王琦, 陈乐华,等. 基于扫描光纤激光器的光纤传感解调仪研究[J]. 光子学报,2009, 38(1): 82-86.

[16] ZHOU Chunxin, ZENG Qingke, QIN Zixiong, et al. Principle and progress of fiber grating strain-temperature sensors [J]. Laser & Optoelectronics Progress, 2006, 43(10): 53-58.
周春新, 曾庆科, 秦子雄, 等. 光纤光栅应变-温度传感器的原理及进展[J]. 激光与光电子学进展, 2006, 43(10): 53-58.

[17] LIU Jingwang, DU Zhenhui, LI Jinyi, et al. An analytical model for the tuning characteristics of the static, dynamic, and transient behavior on temperature or injection current of DFB laser diodes[J]. Acta Physica Sinica, 2011, 60(7): 353-357.
刘景旺, 杜振辉, 李金义, 等. DFB激光二极管电流-温度调谐特性的解析模型[J]. 物理学报, 2011, 60(7):353-357.

[18] JIANG Peng. Research on high-power laser modulation system and technology for FM/CW imaging lidar[D]. Harbin: Harbin Institute of Technology, 2010.
姜鹏. FM/cw激光成像雷达中的大功率激光调制系统及技术研究[D]. 哈尔滨: 哈尔滨工业大学, 2010.

[19] SHI Y, LI S, CHEN X, et al. High channel count and high precision channel spacing multi-wavelength laser array for future PICs[J]. Scientific Reports, 2014, 4(1): 1-6.

[20] LIU Jie, ZHAO Hong, WANG Peng, et al. An optical current transformer based on DFB laser [J]. Journal of Opto-electronics Laser, 2011, 22(12):1789-1792.
刘杰, 赵洪, 王鹏, 等. 基于DFB激光器解调技术的光学电流互感器[J]. 光电子激光, 2011, 22(12):1789-1792.

[21] LEAL A G, FRIZERA A, MARQUES C. Thermal and mechanical analyses of fiber Bragg gratings-embedded polymer

diaphragms[J]. IEEE Photonics Technology Letters, 2020, (99):1-1.
[22] YU Q, ZHANG Y, DONG Y, et al. Study on optical fiber Bragg grating temperature sensors for human body temperature monitoring[C]. 2012 Symposium on Photonics and Optoelectronics, IEEE, 2012.
[23] LI Y, LU B, REN L, et al. A highly precise FBG sensor interrogation system with wavemeter calibration[J]. Optical Fiber Technology, 2019, 48(1):207-212.

FBG Sensor System without Wavelength Correction Based on REC-DFB Tunable Laser

DENG Wei[1,2], DAI Pan[2], WANG Feng[2], GE Hantian[2], CHEN Xiangfei[2]
(1 *College of Network and Communication, Nanjing Institute of Information Technology, Nanjing* 210023, *China*)
(2 *College of Engineering and Applied Sciences, Nanjing University, Nanjing* 210023, *China*)

Abstract: With the rapid development of optical fiber communication and optical fiber sensing, the Fiber Bragg Grating (FBG) sensor has become one of the fastest growing and most widely used optical fiber sensors. Owing to the FBG sensor has many advantages in terms of compact size, low cost, wavelength-encoded, anti-electromagnetic interference, easy multiplexing and so on, it has attracted great interests in the field of sensing and been widely used in medical healthcare, pressure detection, battery safety condition and building structural health monitoring. FBG sensors demodulate parameters such as strain, vibration and temperature by detecting the changes of FBG reflection wavelength, with the aid of core technology of laser source and demodulation method. However, the current Tunable Distributed Feedback (DFB) lasers for optical communication applications often have narrow tuning range and low tuning speed, and require additional auxiliary wavelength reference when directly used for FBG sensor demodulation system, which makes the system complex and affects its practicability. Therefore, there is still no tunable laser source with simple structure and low cost that is specifically suitable for FBG sensing systems.

In this paper, a wavelength correction-free FBG sensing system was proposed to identify the wavelength changes and demodulate the temperature changes of the FBG sensor without wavelength correction of the wavelength-swept DFB laser based on Reconstruction Equivalent Chirp (REC) technique. As one of the most significant wavelength tunable laser sources, the DFB semiconductor laser has the characteristics of high reliability, low noise, fast response, high output power, good repeatability, and simple tuning scheme. Compared with many other tunable lasers with different realization schemes, the fabrication process of DFB laser is the best choice for both cost and applicability. The DFB laser used in this paper was designed and fabricated using a special process method-REC technique. By sampling the seed grating with uniform period, the low-cost submicron holographic exposure technique of laser chip fabrication can achieve the same wavelength accuracy as the high-cost nanometer electron beam lithography technique while retaining its intrinsic characteristics. When a tunable DFB laser is selected as the laser source for an FBG temperature sensing system, the temperature information can be demodulated by reading the voltage signal of the optical signal reflected by the FBG through the Photodetector (PD). In the wavelength-swept-based FBG sensing demodulation system, the only data that can be obtained directly from the Oscilloscope (OSC) is the optical intensity of the FBG reflection spectra and the corresponding time in the sweeping cycle of the DFB laser. In order to accurately analyze the external environment changes measured by the FBG sensor from these data, it is necessary to calibrate the relationship between wavelength and time during the wavelength-swept process of DFB laser in advance. Firstly, the instantaneous wavelength is calibrated by the calibration method based on Mach-Zehnder Interferometer (MZI), and the relationship between wavelength and time is obtained. Then in the FBG temperature sensing system based on tunable laser, the FBG sensor is placed in the thermostatic bath with a constant temperature accuracy of 0.1 ℃. In the experiment, the tunable REC-DFB semiconductor laser was used as the wavelength-swept laser source. After the optical signal passed through the circulator, it acted on the FBG sensor for temperature sensing, and then the FBG reflected optical signal was received by the PD and recorded by the OSC. By

using the characteristic that the reflected optical signal reaches maximum when the laser wavelength coincides with the reflection central wavelength of the measured FBG, and then using the relationship between wavelength and time in the laser sweeping cycle that has been calibrated, the wavelength corresponding to the maximum output signal of the FBG demodulation system is extracted. Finally, by detecting the wavelength offset of the reflected FBG, the measured changes of external temperature can be linearly demodulated even when the laser wavelength changes are nonlinear.

Experimental results show that the proposed wavelength-correction-free FBG sensing system can perform accurate temperature detection in the range of 200 ℃, and the coefficient of determination (R^2) of linear fitting relationship between wavelength and temperature is 0.995 6. The linearity of the measured wavelength and temperature is good, with the $1-R^2$ of only 0.004 4. The laser source of sensing system can be tuned up to 2.5 nm with 1 kHz sawtooth wave modulation, and no additional wavelength correction device is required for the measurement process.

Key words: Fiber Bragg grating; Reconstruction equivalent chirp technique; Distributed feedback laser; Wavelength correction free; Tunable laser

OCIS Codes: 060.3735; 060.2370; 280.4788; 140.3490; 140.3600; 140.5960

Foundation item: National Natural Science Foundation of China(No. 61975076), Chinese National Key Basic Research Special Fund(Nos. 2018YFA0704402, 2018YFB2201801, 2018YFE0201200)